



Multi-Response Optimization and Surface Integrity Characteristics of Wire Electric Discharge Machining α -Phase Ti-6242 Alloy

Prasanna R¹ · Kavimani V¹ · Gopal P.M¹ · Simson D²

Received: 30 September 2020 / Revised: 17 May 2021 / Accepted: 19 May 2021 / Published online: 5 June 2021
© The Author(s), under exclusive licence to Springer Nature Singapore Pte Ltd. 2021

Abstract

The current research aims to optimize wire electric discharge machining parameters with multi-objectives while machining contemporary titanium alloy. Wire electric discharge machining analysis was conducted by varying the key machining parameters, viz. pulse ON time, pulse OFF time, voltage and wire feed rate. Based on preferred parameters, Taguchi orthogonal array is designed and the optimal parameter combination for minimal surface roughness and material removal rate is identified. Results reveal that material removal rate increases with increase in pulse ON time and surface roughness found to be minimized with increase voltage and wire feed rate. Multi-objective optimization was carried through Technique for Order of Preference by Similarity to Ideal Solution methodology that helps in attaining optimal combination that results in maximum material removal rate (2.84 mm³/min) and minimum surface roughness (2.43 μ m). Traces of deterioration and deep crater were observed over the machined surface when machining parameters like voltage and pulse ON time are high.

Keywords Ti-6242 · WEDM · TOPSIS · MRR · Surface roughness

Introduction

Titanium-based alloys recently perceived interest in transport industries due to their unique properties such as better strength, high fracture toughness, low thermal conductivity, high oxidation and corrosion resistance (Li et al. 2019; Lu et al. 2019). Among the available titanium alloys, Ti-6242 (6Al-2Sn-4Zr-2Mo) alloy has high strength-to-weight ratio compared to steel; this fact made them a favourable material for high-temperature aerospace application (Guo et al. 2012; Xiao et al. 2018). These alloys are mostly used to develop super plastic formed parts and also used as casing

material for automotive and aerospace components, viz. exhaust nozzles, engine disc and turbine blades (Ahmadnia et al. 2019; Liu and Chen 2019). Whatsoever, high toughness and high strength of these alloys make it difficult to machine and shape them to a specified size and shape. This fact act as a major barrier for extensive application of this alloy in terms of high machining cost (Shi et al. 2016; Varote and Joshi 2017).

Machining of these alloys by conventional machining approach has several problems such as galling and smearing along cutting edges of tool and these facts result in rapid failure (damage) of cutting tools. Ti alloys are known for poor thermal conductivity and owing to this factor heat developed during conventional machining, viz. turning, milling remains focused near the cutting zone that leads to cutting tool failure (Sartori et al. 2018; Touazine et al. 2019). Likewise, high-speed machining of Ti-based alloys is not possible since the upper speed limit is 350 surface feet/min and above this range, several damages will occur over the surface of metal layers. Further increase in cutting speed results in surface damages. Hence, there is a need of alternate machining process to reduce the machining cost (Ezilarasan and Velayudham 2013; Singh and Pandey 2013). In recent days, some researchers adopt unconventional machining process, viz. abrasive water jet machining and wire electrical

✉ Prasanna R
prasannaravi.g@gmail.com

Kavimani V
manikavi03@gmail.com

Gopal P.M
gopal33mech@gmail.com

Simson D
adsimson@gmail.com

¹ Department of Mechanical Engineering, Karpagam Academy of Higher Education, Coimbatore, India

² Discipline of Mechanical Engineering, Indian Institute of Technology, Palakkad, India

discharge machining (WEDM) in order to reduce the usage of high expensive conventional machining process and to reduce material waste. However, equipment cost and workpiece height are major limitations for these unconventional machining techniques. Based on this perspective, WEDM was considered a better option for machining Ti-based alloys (Bisaria and Shandilya 2020; Jahan and Alavi 2019; Khosravifar et al. 2018).

WEDM process works based on electro thermal erosion process that assists to machine the complex dimension components such as gears, dies and press tools. Conversely, WEDM processes have limitations in machining Ti-based alloy. Herein, debris produced near machining gap was difficult to remove which made them unsteady during the machining process. These Ti-based alloys have low thermal conductivity that forms recast layer-based problems. In some cases, melting and re-solidification of material form thin coating over material surface and this fact alters the unique properties of materials. Further, heat-affected zone over the material surface will also decrease the machinability of Ti-based alloys. Based on these evidence, there is a need of hour to explore the machinability of Ti-based alloys (Mahapatra and Amar 2006; Muralova et al. 2018; Sarkar et al. 2008).

There are only few researches reported concerning the possibility of WEDM process over Ti-based alloys. Further, there is a demanding necessity for optimizing the machining parameters of WEDM. Advancement in soft computing technique results in the formation of various optimization technique that includes artificial neural networks, genetic algorithm, ant colony algorithm, grey relation analysis, technique for order of preference by similarity to ideal solution (TOPSIS) and response surface methodology (Huu-Phan et al. 2019; Huu et al. 2019; Nguyen et al. 2020). Among the available methodology, TOPSIS-based technique was widely preferred by the researchers to solve difficult problems in a minimal duration of time. Pulse ON time (TON), pulse OFF time (TOFF), servo voltage (V), peak current (PC), wire tension (WT), wire feed rate (WFR), pulse peak voltage and water pressure are the common available machining parameters for WEDM process (Gopal et al. 2018; Kavimani et al. 2019a, b). There are only few researches that are done based on WEDM of titanium-based alloys. Sivaprakasam and co-workers adopted genetic algorithm-based response surface methodology to investigate the micro-machining behaviour of Ti-6Al-4V alloy (Sivaprakasam et al. 2014). They

investigated the influence of machining parameters, viz. voltage, capacitance and feed rate over output response, viz. Kerf width, material removal rate (MRR) and surface roughness (Ra). Results reveal that voltage and feed rate are the most influencing parameter for MRR. Taguchi method was utilized by Rupesh et al. to optimize the WEDM parameter of pure Ti (Chalisingaonkar and Kumar 2013). The adopted input parameters are TON, TOFF, V, WT, WFR and PC and studied its influence over Ra and observed that TON is the major influence parameter for output response. Mustufa et al. adopted multi-objective genetic algorithm to understand the machinability behaviour of Ni-Ti alloy. The selected parameters are discharge voltage, capacitance and electrode material, viz. brass, Tungsten as the input parameter; tool wear rate and MRR as the output response. It was observed that brass-based electrode material exhibits minimal tool wear (Abidi et al. 2018).

Based on a clear-cut literature survey, TON, TOFF, WFR, and V are the most influencing parameters for WEDM. There are only few literatures based on WEDM studies on Ti-based alloy and machinability behaviour (WEDM studies) of Ti-6242 alloy was not yet reported from the available literatures. Based on this evidence, an attempt has been made to explore the WEDM characteristics of Ti-6242 alloy by adopting TOPSIS technique to determine the optimal values of process parameters and SEM topography analysis has been performed to study the machined surface.

Experimental Details

The material composition of Ti-6242 alloy is given in Table 1. Grade 6Al 2Sn 4Zr 2Mo titanium alloy is a near alpha phase alloy that has been developed to sustain the mechanical strength and corrosion resistance at elevated temperature used in engineering application up to 811K. In this study, Ti-6Al-2Sn-4Zr-2Mo is machined by CNC wire electro discharge machining and samples were prepared in the dimension of 10*10*5 mm as suitable for measuring surface roughness. The experiments were performed on a high precision EXETEK EX40, WEDM machine with brass of diameter 0.25 mm as the wire material was majorly preferred as the tool electrode. De-ionized water was used as dielectric fluid for experiment and acts as a carrier agent for debris produced during WEDM. The machine specification of WEDM is given in Table 2.

Table 1 Material composition of Ti-6Al-2Sn-4Zr-2Mo alloy

Ti	Al	Sn	Zr	Mo	Fe	O	Si	C	N	H
83.785–87.24	83.785–87.24	1.8–2.2	3.6–4.4	1.8–2.2	0.25 (max)	0.15 (max)	0.060–0.10	0.050(max)	0.050(max)	0.015(max)

Table 2 Machine specification

Job size acceptable	400 × 500 × 200 mm
Max taper cutting angle	± 30° on 50 mm job
Wire diameter	0.25 mm
Wire material	Brass
Max wire spool capacity	6 kg
Max cutting speed	120 mm/min
Axis controls available	X, Y, U, V
Flushing rate	12 lpm
Dielectric medium	De-ionized water
Wire tension	0.2–1.25 kg
Dielectric temperature	22–25 °C

Influence of input process parameter of WEDM was analysed at various levels. The machining factors and their parametric range were chosen based on literature and experience which are given in Table 3. After machining, the sample piece was taken to analyse MRR and surface roughness. The MRR was calculated by using the equation given below (Urtekin 2015).

$$\text{Material Removal Rate} = F \times D_w \times T \text{ mm}^3/\text{min} \quad (1)$$

where F is the cutting speed (mm/min), Dw is the width of cut (mm) and T is the thickness of the workpiece (mm).

Mitutoyo SJ-310 surface roughness measuring device was used to measure the average surface roughness of WEDM machined samples. The measurement was done with three repetitions at a range of 5 mm from prime, centre and bottom of the machined surface and its average was taken for study.

With four process parameters at three levels, L27 orthogonal array is chosen as per Taguchi method to minimize the experiment numbers and to determine the optimum level of each process parameter.

Results and Discussion

The obtained results were converted into signal-to-noise ratios and the mean value for each level of all the control factors was calculated. The experimental results and corresponding S/N ratio were given in Table 4. In this research,

maximum MRR and minimum surface roughness are considered as a better result; thus, the larger the better S/N ratio is used for MRR and the smaller the better S/N ratio is used for surface roughness. Then mean table and main effect plot for surface roughness and material removal rate are plotted.

Effect of WEDM Factors on Material Removal Rate

The effect of each parameter over MRR can be seen in Fig. 1 and Table 5. The relationship between all these operating parameters and response (MRR) is shown in Fig. 2. In Figs. 1 and 2, it can be visualized that increase in TON and decrease in TOFF increase MRR. As TON increases, the sparking time gets increased which helps to increase the material removal that leads to higher MRR. Decrease in TOFF leads to increased sparking time and reduced idle time which results in higher MRR (Bisaria and Shandilya 2019).

It is elucidated that MRR gets improved as servo voltage increased due to higher spark energy. So, MRR is found to be increasing as voltage value increases as a result of rise in spark energy across electrode gap. Speeding up the WFR leads to increase in MRR initially and it reduces the MRR for further increase. In general, increase in WFR leads to wire breakage and reduces the machining time and sparking time which leads to lower MRR.

In Fig. 2, it was found that increase in V and TOFF leads to increased MRR. Increase in V helps to rise in spark energy which helps to penetrate the material easily that leads to increase in material removal rate. Interaction effect of each parameter over the MRR is also given in Fig. 2a–d for further understandings. The optimal levels of process parameter of WEDM for attaining maximum MRR are spark time TON 6 (µs), TOFF 6 (µs), voltage 50 (V) and WFR 4 (mm/min). The interaction plot for MRR is depicted in Fig. 3 where each plot exhibits the interaction between four different machining parameters like TON, TOFF, V and WFR. This infers the influence of one factor is dependent upon another factor.

All the parameters like TON, TOFF, V and WFR are found as significant over MRR as given in ANOVA for MRR Table 6 (since P-value < 0.05). V contributes more than other parameters of the process (since Seq SS = 0.079151 value is higher than other process parameters). In this study, MRR gradually increased by increasing spark time and V,

Table 3 WEDM parameters and their values at different levels

S. No	Factor	Unit	Notation	Levels		
				L1	L2	L3
1	TON	µs	A	4	5	6
2	TOFF	µs	B	6	8	10
3	V	V	C	50	65	80
4	WFR	m/min	D	2	4	6

Table 4 Experimental plan and signal to noise ratio of samples

Run	Input parameter				Output response		S/N ratio	
	TON (μ s)	TOFF (μ s)	Voltage (V)	WFR (m/min)	MRR (mm^3/min)	Ra (μm)	S/N ratio for MRR	S/N ratio for Ra
1	4	6	50	2	2.5716	2.4219	8.20407	-7.68312
2	4	6	65	4	2.6822	2.4826	8.56982	-7.89814
3	4	6	80	6	2.7635	2.5537	8.82919	-8.14340
4	4	8	50	4	2.5720	2.4420	8.20542	-7.75491
5	4	8	65	6	2.6210	2.4510	8.36934	-7.78687
6	4	8	80	2	2.6530	2.4820	8.47474	-7.89604
7	4	10	50	6	2.5420	2.3959	8.10351	-7.58937
8	4	10	65	2	2.5710	2.4254	8.20204	-7.69567
9	4	10	80	4	2.6820	2.4710	8.56918	-7.85745
10	5	6	50	2	2.6130	2.4720	8.34279	-7.86097
11	5	6	65	4	2.6780	2.5620	8.55621	-8.17158
12	5	6	80	6	2.7650	2.6040	8.83390	-8.31282
13	5	8	50	4	2.5920	2.4614	8.27270	-7.82364
14	5	8	65	6	2.6880	2.5112	8.58859	-7.99763
15	5	8	80	2	2.7260	2.5230	8.71052	-8.03835
16	5	10	50	6	2.5514	2.4720	8.13557	-7.86097
17	5	10	65	2	2.6423	2.4610	8.43964	-7.82223
18	5	10	80	4	2.7428	2.5170	8.76388	-8.01766
19	6	6	50	2	2.6910	2.4770	8.59827	-7.87852
20	6	6	65	4	2.7570	2.5460	8.80874	-8.11717
21	6	6	80	6	2.7940	2.5946	8.92453	-8.28141
22	6	8	50	4	2.6915	2.5020	8.59989	-7.96575
23	6	8	65	6	2.6727	2.5330	8.53900	-8.07270
24	6	8	80	2	2.7636	2.5420	8.82950	-8.10351
25	6	10	50	6	2.6410	2.4921	8.43537	-7.93131
26	6	10	65	2	2.6510	2.4928	8.46819	-7.93375
27	6	10	80	4	2.7640	2.5432	8.83076	-8.10761

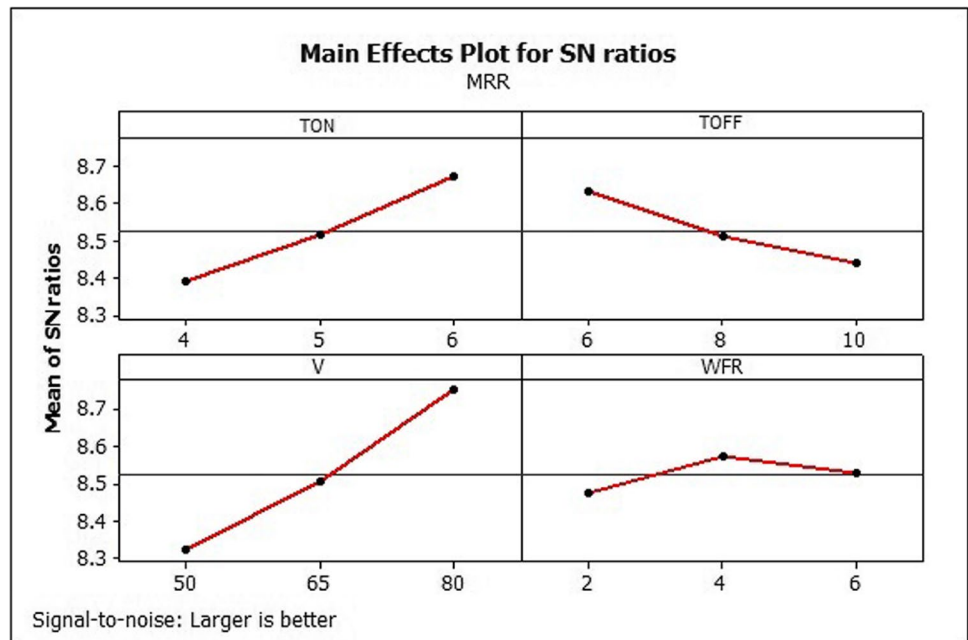
Fig. 1 Main effect plot for MRR of Ti alloy

Table 5 Response table for material removal rate

Level	TON	TOFF	V	WFR
1	8.339	8.630	8.322	8.474
2	8.516	8.510	8.505	8.575
3	8.670	8.439	8.752	8.529
Delta	0.279	0.191	0.430	0.101
Rank	2	3	1	4

decreasing the rest time and WFR. Large spark discharge time and high voltage which generate high temperature at shorter span which melts and vaporizes the metal at high rate that increases the MRR.

$$C5 = 2.4937 + 0.0426389 A - 0.0293222 B + 0.0660222 C + 0.00867222 D$$

Effect of WEDM Factors on Surface Roughness

Figure 4 clearly indicates the influence of considered parameters over surface roughness and the relation between V, WFR, TON and TOFF with surface waviness is shown in

Fig. 5. In Figs. 4 and 5, it can be visualized that increase in V and TON results in decrement in surface roughness value. Increase in V and TON results in rise in spark energy across electrode gap that removes more material and the surface becomes rough. Increase in WFR provides the fresh wire which crosses over the machining area offers higher energy spark that result in formation of craters in the surface (Shandilya et al. 2018) (Table 7).

Higher TOFF gives more time to vanish the molten material in the machined surface that avoids the formation of re-solidification layer. So the surface finish is high when TOFF is fixed as high. Surface roughness can be minimized by increasing the TOFF and maintaining low value for other parameters. Interaction effect of each parameter over the

roughness is also given in Fig. 6 for further understandings. The optimal level for obtaining minimum surface roughness is TON 4 (μs), TOFF 10 (μs), V 50 (V) and WFR 2 (m/min).

ANOVA for surface roughness (Ra) is given in Table 8 and V is the most significant factor which contributes more

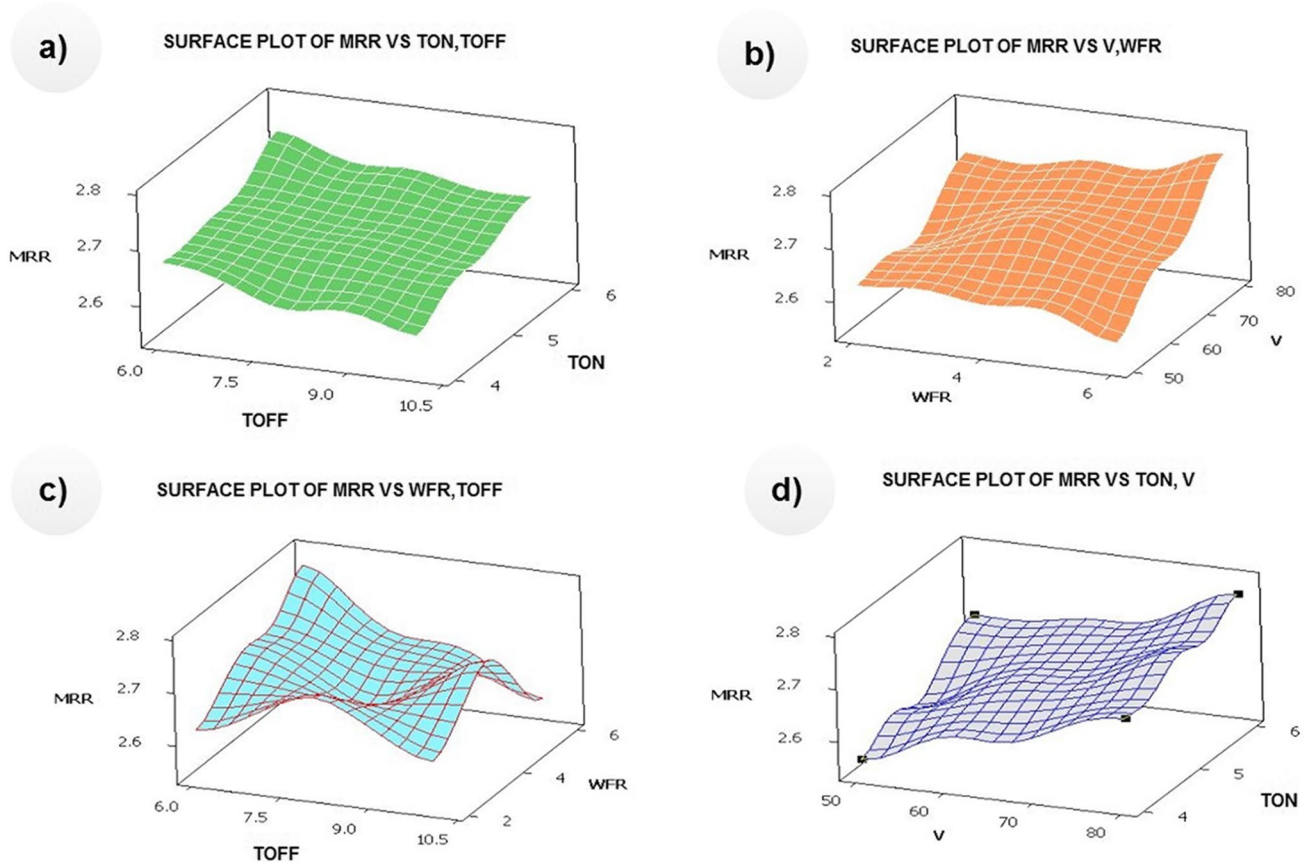
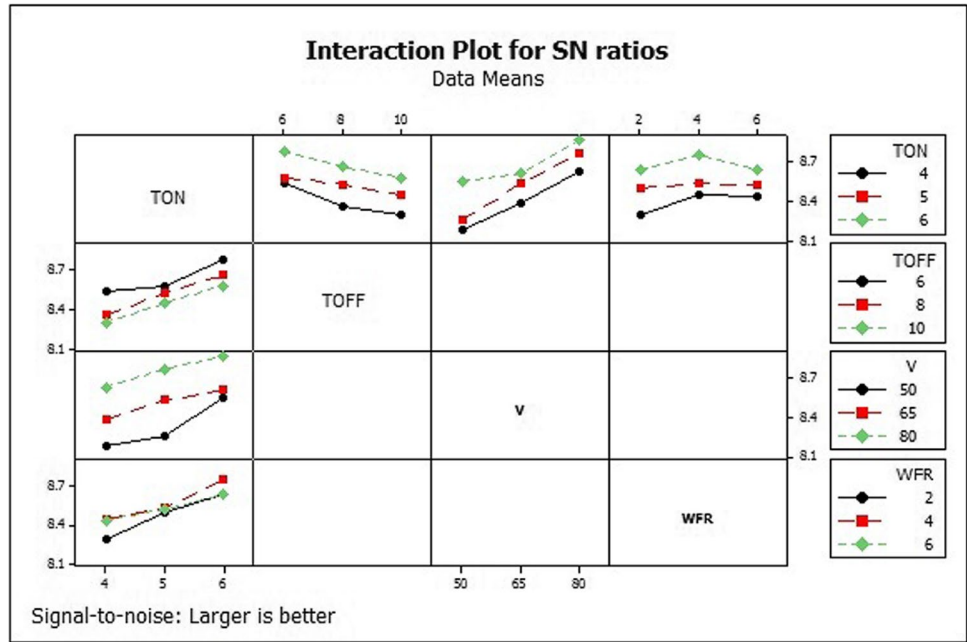


Fig. 2 3D response surface graph for MRR with **a** respect to TON and TOFF, **b** respect to V and WFR, **c** respect to WFR and TOFF and **d** respect to V and TOFF

Fig. 3 Interaction plot for MRR



on surface finish of machined component (since Seq SS (0.026798) value is higher than other process parameters). Herein, servo voltage has the major contribution in influencing the surface roughness.

Step 2: A matrix has to be developed on the basis of all accessible data about material’s attributes (decision matrix). Step 3: Normalized decision matrix, R_{ij} , can be obtained as described below:

$$C6 = 2.36876 + 0.0331778 A - 0.0246333 B + 0.0385667 C + 0.0172444 D$$

Multi-Objective Optimization Using TOPSIS

In this research, multiple performance characteristics are analysed using techniques for order performance by similarity to ideal solution. In this method, multiple performance characteristics are converted into ideal coefficients.

$$r_{ij} = \frac{x_{ij}}{\sqrt{\sum_{i=1}^m x_{ij}^2}} \quad j = 1, 2, \dots, \dots, n \quad (2)$$

where x_{ij} is the performance of i th alternative in relation to j th attribute, r_{ij} stands for normalized value, $i = 1 \dots m$ and $j = 1 \dots n$, x_{ij} denotes the actual value of the i th value of the experiment no. j .

Steps in TOPSIS Analysis

Step 1: Determine the objective and pertinent assessment attributes.

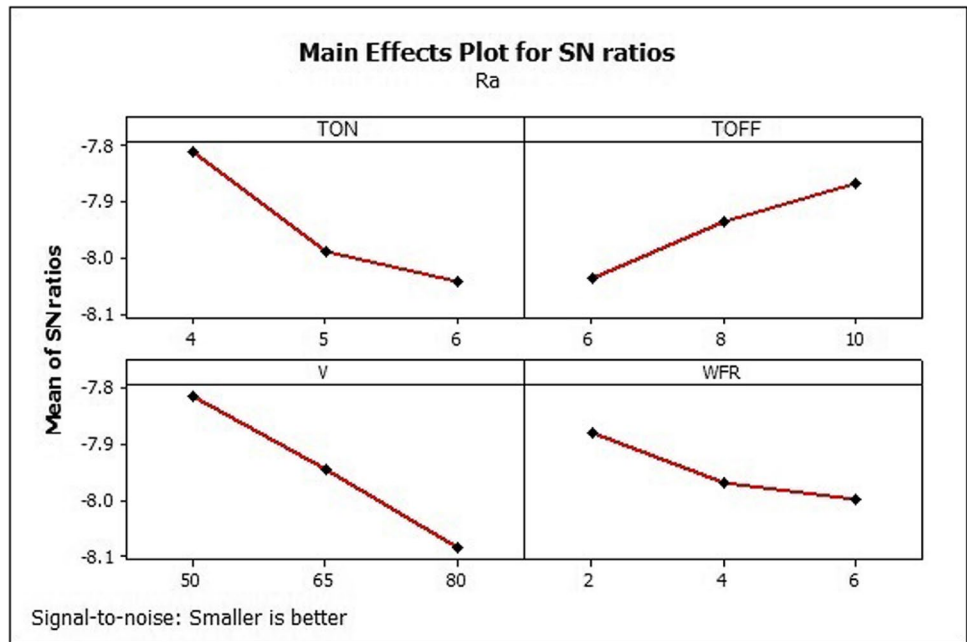
Step 4: Multiplying the normalized decision matrix with its associated weights the weighted normalized decision matrix is formed as

Table 6 Analysis of variance for MRR

Source	DF	Seq SS	Adj SS	Adj MS	F-test	P-value	Cont. %
TON	2	0.032866	0.032866	0.016433	30.66	0	23.16
TOFF	2	0.015856	0.015856	0.007928	14.79	0	11.17
V	2	0.079151	0.079151	0.039575	73.84	0	55.79
WFR	2	0.004345	0.004345	0.002172	4.05	0.035	3.062
Error	18	0.009647	0.009647	0.000536			
Total	26	0.141864					

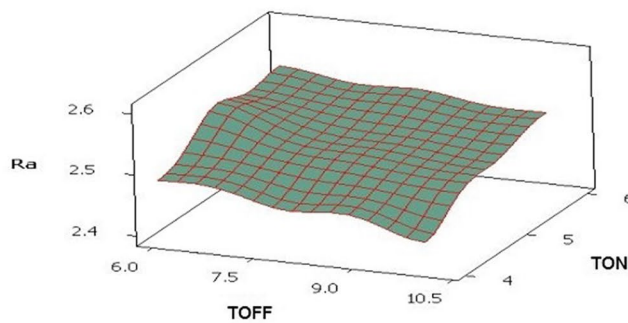
R-Sq = 93.20% R-Sq(adj) = 90.18%

Fig. 4 Influence of WEDM parameters on surface roughness



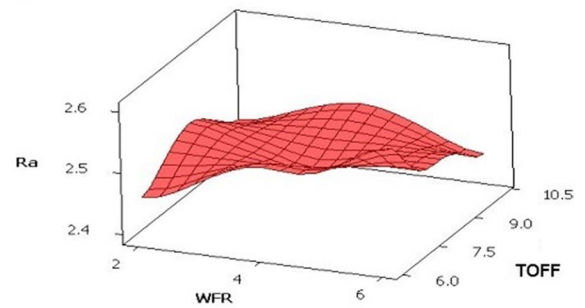
a)

SURFACE PLOT OF Ra VS TON, TOFF



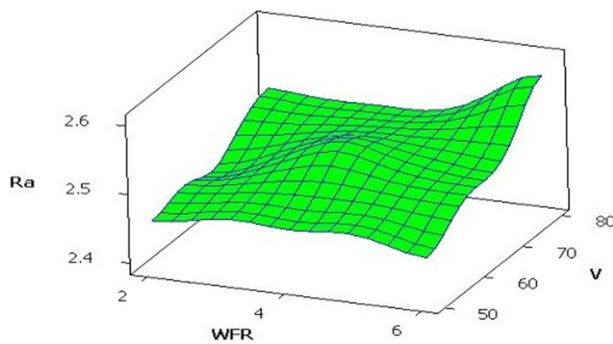
b)

SURFACE POT OF Ra VS TOFF, WFR



c)

SURFACE POT OF Ra VS V, WFR



d)

SURFACE PLOT OF Ra VS TOFF, V

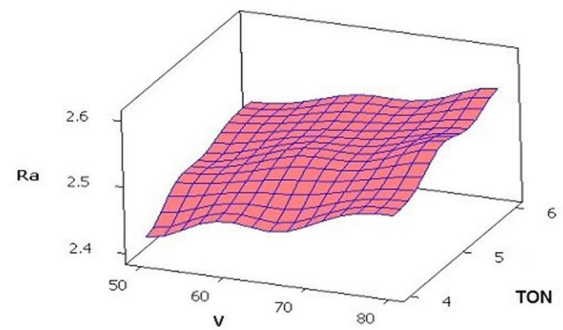


Fig. 5 3D response surface graph for surface roughness with **a** respect to TON and TOFF, **b** respect to TOFF and WFR, **c** respect to V and WFR and **d** respect to TON and V

Table 7 Response table for Ra

Level	TON	TOFF	V	WFR
1	- 7.812	- 8.039	- 7.817	- 7.879
2	- 7.99	- 7.938	- 7.944	- 7.968
3	- 8.044	- 7.868	- 8.084	- 7.997
Delta	0.232	0.17	0.268	0.118
Rank	2	3	1	4

$$V = W_{ij}r_{ij}$$

where $i = 1 \dots m$ and $j = 1 \dots n$. w_j denotes the weight of the j th attribute.

Step 5: Positive (V^+) and negative (V^-) ideal solutions were determined as given

$$V^+ = \sum_i^{max} v_{ij} | j \in J . \sum_i^{min} | j \in J | i = 1, 2, \dots, m \tag{3}$$

$$= V_1^+, V_2^+, V_3^+, \dots, V_n^+$$

$$V^- = \sum_i^{min} v_{ij} | j \in J . \sum_i^{max} | j \in J | i = 1, 2, \dots, m \tag{4}$$

$$= V_1^-, V_2^-, V_3^-, \dots, V_n^-$$

Step 6: Calculate the separation measures - the separation of each alternative from ideal one. In this step,

the distances of each alternative from negative ideal solution (S_i^-) and positive ideal solution (S_i^+) are calculated

$$S_i^+ = \sqrt{\sum_{j=1}^n (v_{ij} - v_j^+)^2} \quad i = 1, 2, \dots, n \tag{5}$$

$$S_i^- = \sqrt{\sum_{j=1}^n (v_{ij} - v_j^-)^2} \quad i = 1, 2, \dots, n \tag{6}$$

Step 7: In this phase, the comparative proximity of a specific option to the optimal solution is expressed as follows:

$$CC = \frac{S_i^-}{S_i^+ - S_i^-} \tag{7}$$

Step 8: Rank preference order: The alternative with the highest Closeness Coefficient (CC) is the best choice.

Initially, the responses such as MRR and surface roughness were standardized using Eq. (2) and equal priority is given for both MRR and surface roughness while assigning weights. Normalized weighted values were obtained by multiplying the weight of the particular response and normalized values. Positive and negative ideal solutions found

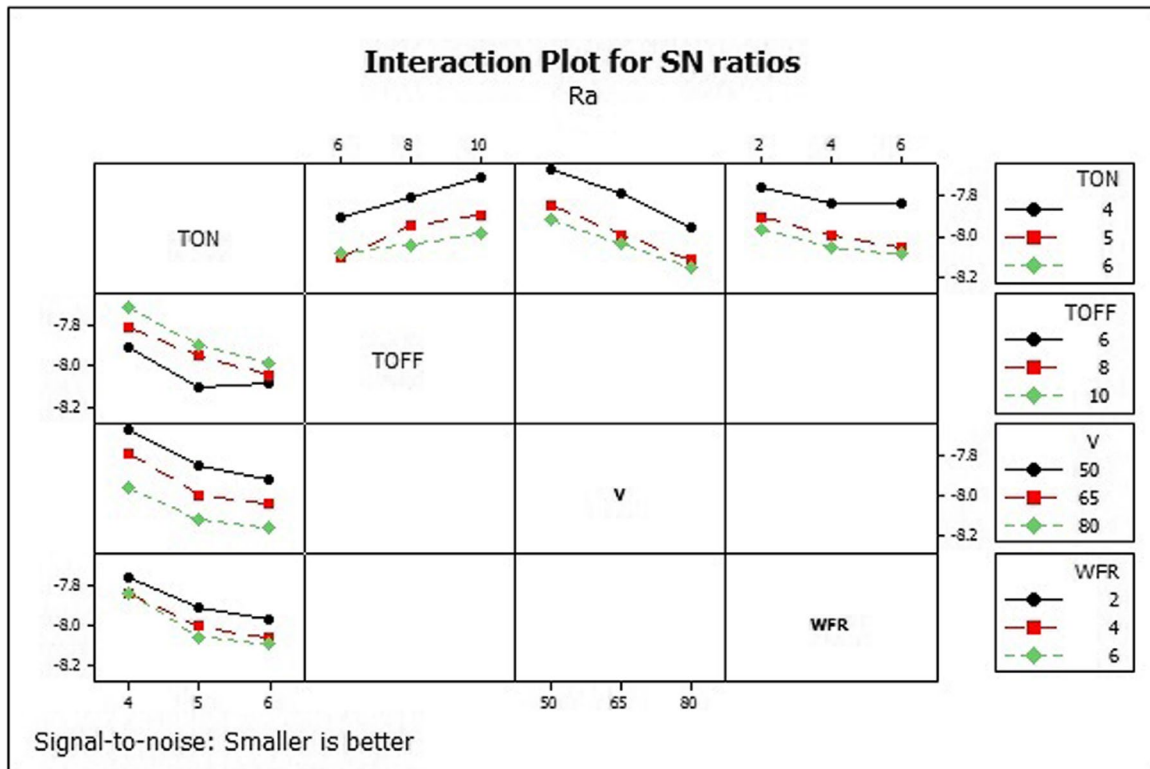


Fig. 6 Interaction plot for surface roughness

Table 8 ANOVA for surface roughness

Source	DF	Seq SS	Adj SS	Adj MS	F-test	P-value	Cont.%
TON	2	0.021698	0.021698	0.010849	52.41	0	31.41
TOFF	2	0.011069	0.011069	0.005535	26.74	0	16.02
V	2	0.026798	0.026798	0.013399	64.73	0	38.80
WFR	2	0.005768	0.005768	0.002884	13.93	0	8.35
Error	18	0.003726	0.003726	0.000207			
Total	26	0.06906					
R-Sq = 94.60% R-Sq(adj) = 92.21%							

are 0.221124 and 0.259322 for MRR wherein 0.281264 and 0.232816 for surface roughness. The separation measures of each criterion from positive and negative ideal solutions are calculated using Eqs. (5) and (6). Further, for all the experimented combinations, CC values are computed with the aid of Eq. (7) and presented in Table 9. Among the 27 experiments conducted, the experiment order 18 is found as optimal parameter combination for better MRR and minimal surface roughness based on the CC values.

The main effect plot is plotted based on the closeness coefficient values obtained from the TOPSIS analysis and is given as Fig. 7. It clearly illustrates the influence of WEDM parameters considered for the current study over closeness coefficient values. The optimum level of each parameter for good surface finish and MRR while machining Titanium alloy is higher pulse ON time, lower pulse OFF time, higher voltage and moderate wire feed rate. The optimal level of parameters is A3B1C3D2 which can be clearly found from the main effect plot. Experiment has been conducted based on the optimal solution acquired from TOPSIS analysis; MRR of 2.84 mm³/min and Ra of 2.43 μm were achieved on WEDM of Ti alloy (Bisaria and Shandilya 2018).

Surface Topography of Machined Surface by Varying Control Parameters

Surface morphology (SEM micrograph) of machined surface with control factor 6 μs pulse on time, 6 μs TOFF, 50 V voltage and 2 m/min WFR is shown in Fig. 8a–d. Formation of surface peak, valley, micro hole, micro crack, deterioration, deep crater and large debris are evidenced from the machined surface of the sample.

This formation is due to the influence of high TON in which the sparking time is high and sparks strike with greater force over the period of time on metal surface that leads to thermal deformations of metal. These facts initiate the formation of deep surface crater over the machined surface [11].

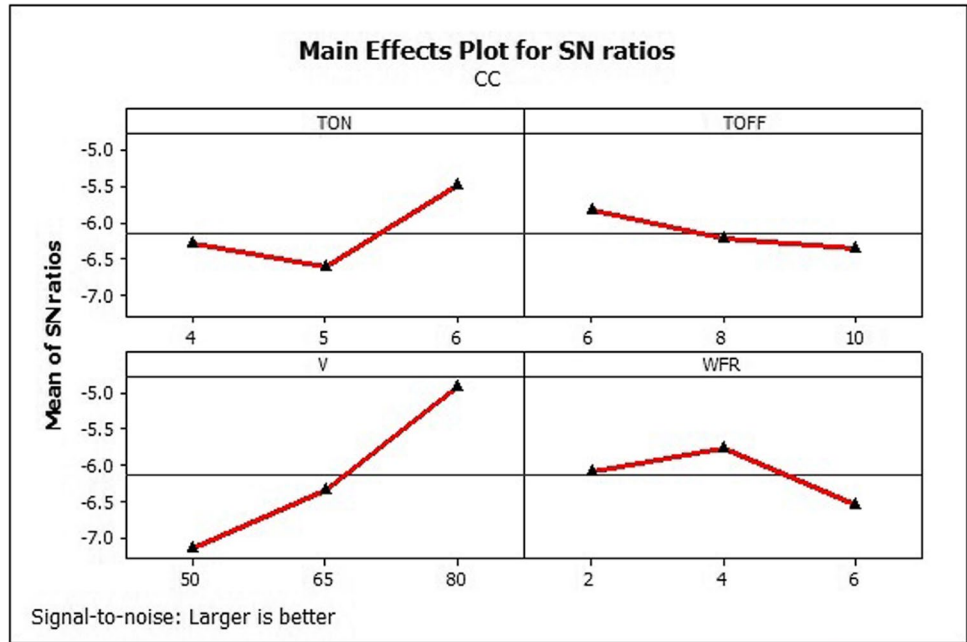
Occurrence of smoother surface is evident from the machined surface (Fig. 9a–d). This might be owed to reasonable TON and voltage in which lower energy sparks

strike over the metal surface uniformly for minimal time that leads to formation of smooth surface. Further higher TOFF allows dielectric fluid to flush the melted materials that make clean and smooth surface. It can be concluded that the process parameter at a reduced and moderate input method achieves better surface roughness than the process parameter at a greater stage.

Table 9 Estimation of separation measures, CC and ranking order obtained from TOPSIS

Experiment No	S+	S-	CC	Rank
1	0.043265	0.033815	0.438705	19
2	0.027424	0.034296	0.555675	10
3	0.0307	0.043111	0.58407	6
4	0.043772	0.030118	0.407609	24
5	0.035285	0.031543	0.471998	16
6	0.032054	0.030274	0.48572	15
7	0.048448	0.038198	0.44085	18
8	0.043453	0.033152	0.432771	22
9	0.026202	0.035722	0.57687	8
10	0.038039	0.027321	0.418008	23
11	0.039107	0.026385	0.402877	25
12	0.040499	0.042681	0.513118	13
13	0.041071	0.027542	0.401411	26
14	0.030222	0.03203	0.514528	12
15	0.027621	0.037669	0.57695	7
16	0.048854	0.02399	0.329335	27
17	0.032113	0.032062	0.499602	14
18	0.025091	0.041174	0.621355	1
19	0.025418	0.036291	0.5881	5
20	0.029517	0.042161	0.588203	4
21	0.038198	0.048448	0.55915	9
22	0.02848	0.033544	0.540819	11
23	0.035333	0.027406	0.436822	21
24	0.028449	0.043621	0.605257	2
25	0.035011	0.027298	0.438107	20
26	0.033467	0.028529	0.46018	17
27	0.028662	0.043643	0.603596	3

Fig. 7 Main effect plot for on closeness coefficient



Conclusion

The influence of control parameter and optimization of WEDM parameter has been made by adopting TOPSIS methodology and the following conclusions are made: Incremental order of TON and V with minimal order of TOFF and WFR results in enhancement of MRR. The surface quality of the machined surface will be enhanced by

increasing the TOFF and other parameters have negative effect over roughness. Optimum machining parameter for achieving high MRR and surface finish at pulse ON time 6µs, pulse OFF time 6µs, voltage 80V, wire feed rate 4 m/min. Surface topography of machined surface shows the evident of craters, surface peak and debris due to effect of control factors.

Fig. 8 SEM images of machined surface at TON = 6 µs, TOFF = 6 µs, V = 50 V, WFR = 2 m/min

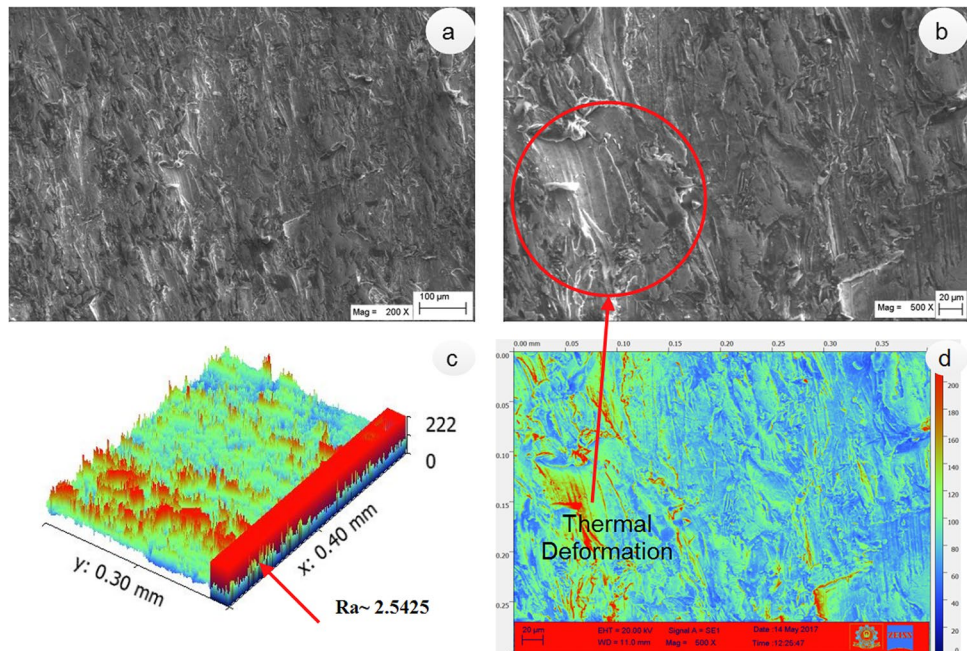
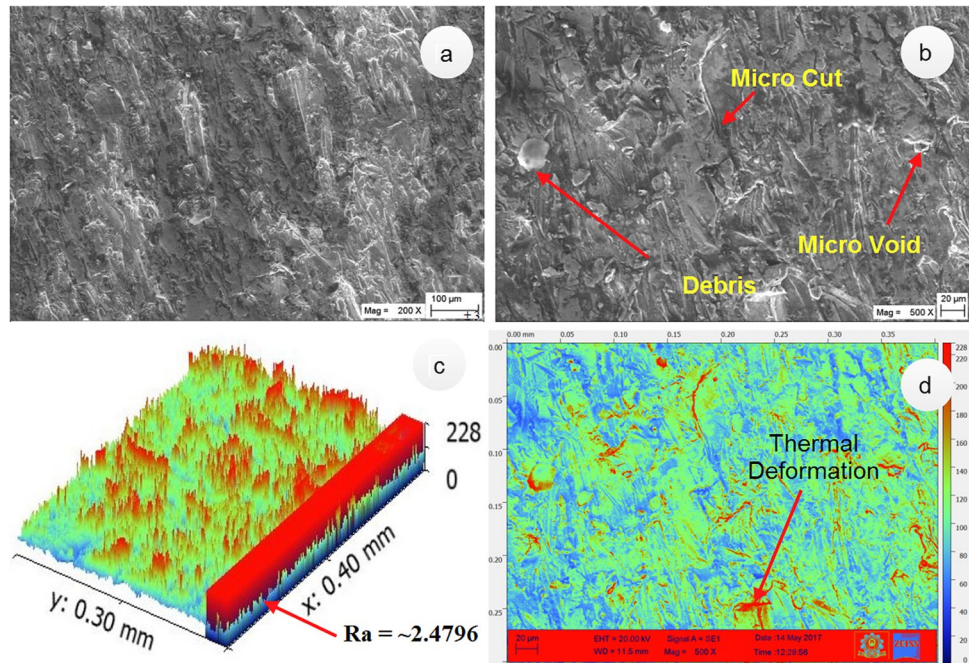


Fig. 9 SEM image of machined surface at TON = 5 μ s, TOFF = 8 μ s, V = 50 V, WFR = 6 m/min



Data Availability The data that support the findings of this article is based on the part of on-going research work, so the data's are not publicly available. Data are however available from the authors upon reasonable request and with permission

Declarations

Conflict of Interest The authors declare no competing interests.

References

- Abidi MH, Al-Ahmari AM, Umer U, Rasheed MS (2018) Multi-objective optimization of micro-electrical discharge machining of nickel-titanium-based shape memory alloy using MOGA-II. *Measurement* 125:336–349
- Ahmadnia S, Aliasghari S, Ghorbani M (2019) Improved electrochemical performance of plasma electrolytic oxidation coating on titanium in simulated body fluid. *J Mater Eng Perform* 28:4120–4127
- Bisaria H, Shandilya P (2018) Study on effect of machining parameters on performance characteristics of Ni-rich NiTi shape memory alloy during wire electric discharge machining. *Mater Today Proc* 5:3316–3324
- Bisaria H, Shandilya P (2019) Study on crater depth during material removal in WEDC of Ni-rich nickel–titanium shape memory alloy. *J Braz Soc Mech Sci Eng* 41:1–11
- Bisaria H, Shandilya P (2020) Surface integrity aspects for NiTi shape memory alloys during wire electric discharge machining: a review. *J Mater Res* 35:537–558
- Chalisingaonkar R, Kumar J (2013) Optimization of WEDM process of pure titanium with multiple performance characteristics using Taguchi's DOE approach and utility concept. *Front Mech Eng* 8:201–214
- Ezilarasan C, Velayudham A (2013) Effect of machining parameters on surface integrity in machining Nimonic C-263 super alloy using whisker-reinforced ceramic insert. *J Mater Eng Perform* 22:1619–1628
- Gopal PM, Prakash KS, Jayaraj S (2018) WEDM of Mg/CRT/BN composites: effect of materials and machining parameters. *Mater Manuf Process* 33:77–84
- Guo Y, Chiu Y, Attallah MM, Li H, Bray S, Bowen P (2012) Characterization of dissimilar linear friction welds of α - β titanium alloys. *J Mater Eng Perform* 21:770–776
- Huu PN, Tien LB, Duc QT, Van DP, Xuan CN, Van TN, Duc LN, Jamil M, Khan AM (2019) Multi-objective optimization of process parameter in EDM using low-frequency vibration of workpiece assigned for SKD61. *Sādhanā* 44:1–11
- Huu-Phan N, Tien-Long B, Quang-Dung L, Duc-Toan N, Muthuralingam T (2019) Multi-criteria decision making using preferential selection index in titanium based die-sinking PMEDM. *J Korean Soc Precis Eng* 36:793–802
- Jahan MP, Alavi F (2019) A study on the surface composition and migration of materials and their effect on surface microhardness during micro-EDM of Ti-6Al-4V. *J Mater Eng Perform* 28:3517–3530
- Kavimani V, Prakash KS, Thankachan T (2019) Influence of machining parameters on wire electrical discharge machining performance of reduced graphene oxide/magnesium composite and its surface integrity characteristics. *Compos Part B Eng* 167:621–630. <https://doi.org/10.1016/j.compositesb.2019.03.031>
- Kavimani V, Soorya Prakash K, Thankachan T (2019) Multi-objective optimization in WEDM process of graphene – SiC-magnesium composite through hybrid techniques. *Meas J Int Meas Confed* 145:335–349. <https://doi.org/10.1016/j.measurement.2019.04.076>
- Khosravifar M, Mirkazemi SM, Taheri M, Golestanifard F (2018) Effect of TiN addition on 3Y-TZP ceramics with emphasis on making EDM-able bodies. *J Mater Eng Perform* 27:2404–2413
- Li H, Zhao Z, Guo H, Ning Y, Yao Z (2019) Dislocation density-based model for flow behavior of a near- α titanium alloy considering effects of initial lamellar thickness. *J Mater Eng Perform* 28:2477–2487

- Liu J, Chen H (2019) Experimental study on microstructure and hardness of pure titanium subjected to torsion deformation at different temperatures. *J Mater Eng Perform* 28:4790–4800
- Lu B, Zhang C, Guo Z, Yang F, Wang H, Volinsky AA, You L (2019) High-carbon ferrochrome effects on microstructure and mechanical properties of powder metallurgy titanium alloys. *J Mater Eng Perform* 28:5361–5368
- Mahapatra Swarup, Amar P (2006) Parametric optimization of wire electrical discharge machining (WEDM) process using Taguchi method. *J Braz Soc Mech Sci Eng* 28:422–429
- Mouralova K, Kovar J, Klakurkova L, Prokes T (2018) Effect of width of kerf on machining accuracy and subsurface layer after WEDM. *J Mater Eng Perform* 27:1908–1916
- Nguyen PH, Banh TL, Mashood KA, Tran DQ, Muthuramalingam T, Nguyen DT (2020) Application of TGRA-based optimisation for machinability of high-chromium tool steel in the EDM process. *Arab J Sci Eng* 45:5555–5562
- Sarkar S, Sekh M, Mitra S, Bhattacharyya B (2008) Modeling and optimization of wire electrical discharge machining of γ -TiAl in trim cutting operation. *J Mater Process Technol* 205:376–387
- Sartori S, Pezzato L, Dabalà M, Enrici TM, Mertens A, Ghiotti A, Bruschi S (2018) Surface integrity analysis of Ti6Al4V after semi-finishing turning under different low-temperature cooling strategies. *J Mater Eng Perform* 27:4810–4818
- Shandilya P, Bisaria H, Jain PK (2018) Parametric study on the recast layer during EDWC of a Ni-rich NiTi shape memory alloy. *J Micromanufacturing* 1:134–141
- Shi Q, Tse YY, Muhammad R, Roy A, Silberschmidt VV, Higginson RL (2016) Effect of machining on shear-zone microstructure in Ti-15V-3Cr-3Al-3Sn: conventional and ultrasonically assisted turning. *J Mater Eng Perform* 25:3766–3773
- Singh S, Pandey A (2013) Some studies into electrical discharge machining of Nimonic75 super alloy using rotary copper disk electrode. *J Mater Eng Perform* 22:1290–1303
- Sivaprakasam P, Hariharan P, Gowri S (2014) Modeling and analysis of micro-WEDM process of titanium alloy (Ti-6Al-4V) using response surface approach. *Eng Sci Technol* 17:227–235
- Touazine H, Chadha K, Jahazi M, Bocher P (2019) Characterization of subsurface microstructural alterations induced by hard turning of Inconel 718. *J Mater Eng Perform* 28:7016–7024
- Urtekin L (2015) Experimental investigation of process parameters for WEDM of Ti-6Al-4V/TiN composites. *Sci Eng Compos Mater* 22:685–692
- Varote N, Joshi SS (2017) Microstructural analysis of machined surface integrity in drilling a titanium alloy. *J Mater Eng Perform* 26:4391–4401
- Xiao Y, Liu H, Yi D, Le J, Zhou H, Jiang Y, Zhao X, Chen Z, Wang J, Gao Q (2018) High-temperature deformation behavior of Ti-6Al-2Sn-4Zr-2Mo alloy with lamellar microstructure under plane-strain compression. *J Mater Eng Perform* 27:4941–4954

Publisher's Note Springer Nature remains neutral with regard to jurisdictional claims in published maps and institutional affiliations.